(1*S*,7*S*)-7-METHYL-6,9-DIAZATRICYCLO[6,3,0,$0^{1,6}$]TRIDECANE-5,10--DIONE, A TRICYCLIC SPIRODILACTAM CONTAINING NON-PLANAR AMIDE GROUPS: SYNTHESIS, NMR, CRYSTAL STRUCTURE, ABSOLUTE CONFIGURATION, ELECTRONIC AND VIBRATIONAL CIRCULAR DICHROISM

Petr MALOŇ[a], C.L. BARNESS[b], Miloš BUDĚŠÍNSKÝ[a], Rina K. DUKOR[c], Dick VAN DER HELM[b], Timothy A. KEIDERLING[c], Zdena KOBLICOVÁ[d], Františka PAVLÍKOVÁ[c], Miloš TICHÝ[a] and † Karel BLÁHA[a]

[a] *Institute of Organic Chemistry and Biochemistry, Czechoslovak Academy of Sciences, 166 10 Prague 6, Czechoslovakia*
[b] *Department of Chemistry, University of Oklahoma, Norman, Oklahoma 73019, U.S.A.*
[c] *Department of Chemistry, University of Illinois at Chicago, Chicago, IL 60680, U.S.A.*
[d] *Research Institute for Pharmacy and Biochemistry, 194 04 Prague 9, Czechoslovakia and*
[e] *Prague Institute of Chemical Technology, 166 28 Prague 6, Czechoslovakia*

Received July 8th, 1988
Accepted July 20th, 1988

The title spirocyclic dilactam (1*S*,7*S*)-7-methyl-6,9-diazatricyclo[6,3,0,$0^{1,6}$]tridecan-5,10-dione (*I*), a molecule designed to contain non-planar amide groups, has been synthesized from an optically active precursor of known absolute configuration. The relative and absolute configurations have been determined by X-ray diffraction. The conformation of the compound has been investigated by X-ray, ^{1}H and ^{13}C NMR, electronic and vibrational circular dichroism. The compound possesses moderately non-planar amide groups in the two rings of nonequal geometry. The electronic CD is dominated by inherent chirality of the amide chromophores. The dilactams *I* and *II* ((1*S*,6*S*)-6-methyl-5,8-diazatricyclo[6,3,0,$0^{1,5}$]undecan-4,9-dione – having five-membered rings) exhibit monosignate amide I VCD and strong VCD bands in the mid-ir region.

The fact that the amide group – the basic constituent unit of peptides and proteins – exhibits a non-negligible degree of conformational flexibility is well known (see refs[1,2] for reviews). Significant deviations are often found from ideally planar arrangement of the six atoms forming the amide grouping when a peptide crystal is investigated by X-ray analysis[3]. Simple amides like formamide or N-methylacetamide are deformable around the amide bond – in fact it is not completely clear whether the amide bond in these molecules is planar or not[4-10]. It is therefore of interest to investigate the properties of the non-planar amides, to establish methods of their detection and to find out

answers to three basic problems: (i) whether the non-planarity so often found in the crystalline state of peptides also persists in solution, (ii) whether non-planarity is a natural property of the amide group or merely a consequence of interactions within the intra- or intermolecular environment and (iii) what is the role of non-planar amide groups in biologically active systems. Especially the last mentioned item raises interesting questions since the non-planar amide group is a chiral species capable of adopting enantiomorphous conformations. For example, this feature together with increased basicity of the amide nitrogen might contribute to chiral discrimination in enzyme catalyzed reactions.

The known X-ray studies on amide compounds[3,11] have been extended by our own work on rigid polycyclic lactams derived from the twistane skeleton[12–17]. These provided models to obtain typical properties of a single planar or non-planar *cis*-amide group. The mentioned investigations as well as those of Klyne et al.[18] on 7-membered lactams and those of Boyd et al.[19] on penicillamine derivatives provided some insight about the occurrence of a single non-planar amide unit. Within a non-planar species the distortion from planarity is most visible in the geometry of the amide nitrogen; $\chi_N \neq 0$ (using the angular convention of Winkler and Dunitz[20]). The amide nitrogen becomes partially sp^3 hybridized and the lone electron pair remains approximately aligned with the π-system ($\tau \sim 0$). The bonds from the carbonyl carbon atom retain their planar arrangement ($\chi_C = 0$). In solution, non-planar amides exhibit a significant shift of the amide I frequency towards higher wavenumbers. Inherent chirality of the non-planar amide chromophore manifests itself by intense oppositely signed CD bands belonging to n–π^* and π–π^* electronic transitions. As compared with the planar species, the n–π^* band exhibits a significant red shift. The sign relation of the CD bands to a particular geometry of the amide chromophore is established both experimentally and on the basis of semiempirical optical activity calculations[8,14,19,21]. For the transoid secondary amide group (and also for the tertiary amide treated as a transoid case) and $\chi_N > 0$ this relation predicts a positive-negative pattern for the respective n–π^* and π–π^* CD bands. The reversed rule is valid for the cisoid amide. The relation holds for the single amide chromophore distorted in the manner described above (i.e. small values of τ and χ_C).

The next logical step in the attempt to mimic more closely the situation potentially existing in oligo- and polypeptides is the evaluation of interactions between non-planar amide groups and a comparison of the resulting effects with those exhibited by the isolated chromophore. However it is more difficult to design and synthesize sufficiently rigid model compounds having several distorted amide groups in a homoconjugated sequence, i.e. separated from one another by one carbon atom as in the peptide backbone. Up to this time four types of compounds were examined: 2,5-piperazinediones (see e.g.[22]),

cyclotripeptides[23], bicyclic dilactams derived from decaline[24] and tricyclic spirodilactams *II*–*VII* (refs[25–30]). Among these the tricyclic spirodilactams are probably the most rigid models due to their polycyclic skeleton. On the other hand it is necessary to recognise that they represent a head-to-head connection of both amide groups in contrast to the head-to-tail connection which is characteristic of a polypeptide primary structure. As racemates these compounds have been known for more than 15 years[25–28], however the synthesis of optically active derivatives has succeeded only recently[29,30]. In a previous communication in this series[30] we investigated the optically active dilactams *II*, *III* and *IV* which have only five-membered rings. In this paper we extend the series by including the dilactam *I* having amide groups located in two six-membered rings. This less strained tricyclic system should allow for more planar amide groups and should also allow an investigation into the differences and similarities of the two six-membered lactam rings.

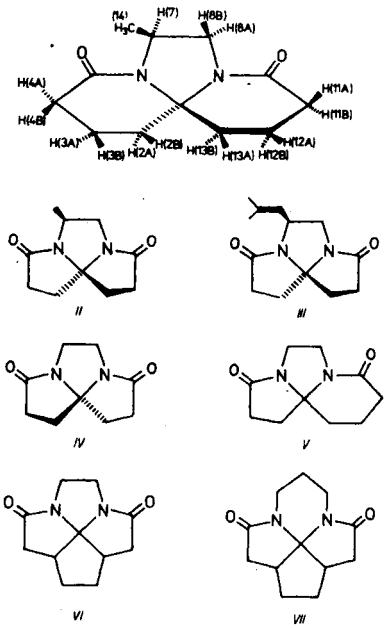

Synthesis of the optically active dilactam *I* is analogous to compounds with five-membered rings i.e. a condensation of diethyl 5-oxononanedioate with (+)-(*S*)-1,2-diaminopropane. Again the reaction provides only one of the two possible diastereoisomers. Its relative configuration was determined by X-ray diffraction and by ^{1}H NMR using hydrogen atoms of the central five-membered ring. To be sure that no bonds to C(2) of the diamine component have been

disrupted in the course of the synthesis, the absolute configuration of *I* was determined by the Bijvoet method. Conformational investigation involved X-ray diffraction as well as NMR and chiroptical methods. In addition to usual electronic circular dichroism spectra we have also recorded circular dichroism in the infra-red using an FTIR VCD spectrometer. Vibrational CD (VCD) spectroscopy shows much promise for detailed stereochemical analysis, thus it is of interest to report preliminary VCD of these amides.

EXPERIMENTAL

(1*S*,7*S*)-7-Methyl-6,9-diazatricyclo[6.3.0.$0^{1,6}$]tridecan-5,10-dione (*I*)

A mixture of diethyl 5-oxononanedioate (0.516 g) and (+)-(*S*)-1,2-diaminopropane (0.16 g) was heated in a sealed tube to 180–190 C for 4 h. The product was crystallized from ethanol–diethyl ether to give 0.19 g (43%) of the pure compound, m.p. 120–122 C. (The melting point was determined on a Kofler block and is uncorrected). Mass spectrum (*m/z*): 222 (M^+), 194, 152, 151, 137. For $C_{12}H_{18}N_2O_2$ (222.28) calculated: 64.84% C, 8.16% H, 12.60% N; found: 64.83% C, 8.33% H, 12.47% N.

Crystal Structure and Absolute Configuration Determination

A crystal with approximate dimensions 0.38 × 0.30 × 0.35 mm was selected for intensity collection. Crystallographic data were collected on a Nonius CAD-4 automatic diffractometer. The space group was determined uniquely as $P2_12_12_1$ from systematic absences. The unit cell dimensions (Table I) were obtained by least squares fit to the $+2\Theta$ and -2Θ values of 48 reflections taken from all octants of reciprocal space, at -135 ± 2 C and at room temperature, using CuK_γ radiation (λ = 1.54051 Å). A total of 1 345 independent reflections with $2\Theta < 150$, 1 320 with $I > 2\sigma(I)$, were measured with Ni-filtered CuK_γ radiation (λ = 1.5418 Å), using the $\Theta-2\Theta$ scan technique. The scan angle used for each reflection was calculated from the formula Θ = (0.90 + 0.14 tan Θ) . The receiving aperture, located 173 mm from the crystal had a variable width, calculated as (3.0 + 0.86 tan Θ) mm, and a constant height of 4 mm. The maximum scan time per reflection was 60 s, with 2/3 of the time spent on the peak and the remaining 1/3 divided equally between the backgrounds. No significant changes were observed in the three standard reflections measured during the course of the data collection. The intensity data were corrected for Lorentz and polarization factors, but

TABLE I
Crystallographic data of the spirodilactam *I* ($C_{12}H_{18}N_2O_2$ (222.29), space group $P2_12_12_1$, Z = 4)

Parameter	-135 ± 2°C	Room temperature
a	10.579(2) Å	10.6394(8) Å
b	13.397(3) Å	13.4479(9) Å
c	7.913(1) Å	8.1130(5) Å
V	1121.5 Å^3	1160.7 Å^3
D_{calc}		1.272 g cm^{-3}

TABLE II
Positional parameters ($\times 10^5$) and isotropic equivalent U ($\times 10^4$) for non-hydrogen atoms of *I*

Atom	*x*	*y*	*z*	*U*
C(1)	38 676(13)	−26 449(9)	82 723(17)	200(6)
C(2)	29 006(13)	−34 617(10)	78 768(20)	254(7)
C(3)	31 568(15)	−43 942(10)	89 441(21)	288(7)
C(4)	36 926(16)	−41 492(10)	107 118(20)	278(7)
C(5)	35 008(12)	−30 813(10)	112 846(19)	228(6)
O(5)	32 075(11)	−28 686(8)	127 397(14)	300(5)
N(6)	37 191(12)	−23 740(8)	100 799(15)	205(5)
C(7)	33 173(14)	−13 264(10)	103 035(18)	235(6)
C(14)	44 257(16)	−6 359(10)	106 872(21)	302(7)
C(8)	27 252(14)	−11 093(10)	85 811(20)	265(7)
N(9)	35 216(10)	−16 988(8)	74 459(16)	226(5)
C(10)	41 054(14)	−12 825(10)	60 893(19)	240(6)
O(10)	38 043(12)	−4 521(8)	55 711(16)	338(5)
C(11)	51 705(15)	−18 589(10)	52 633(18)	265(6)
C(12)	53 981(14)	−29 145(10)	59 094(19)	252(6)
C(13)	52 187(13)	−29 362(10)	78 228(18)	228(6)

TABLE III
Positional parameters ($\times 10^3$) and isotropic thermal parameters (U) ($\times 10^3$) for hydrogen atoms of *I*

Atom	*x*	*y*	*z*	*U*
H(2A)	202(2)	−319(1)	815(2)	24(4)
H(2B)	293(2)	−362(1)	665(2)	29(5)
H(3A)	236(2)	−476(1)	903(3)	40(5)
H(3B)	369(2)	−485(1)	830(2)	29(4)
H(4A)	334(2)	−458(1)	1156(3)	48(6)
H(4B)	456(2)	−429(1)	1074(3)	38(5)
H(7)	274(2)	−131(1)	1126(2)	26(4)
H(14A)	507(2)	−65(1)	971(2)	24(4)
H(14B)	488(2)	−82(1)	1174(2)	42(5)
H(14C)	413(2)	4(1)	1084(3)	31(5)
H(8A)	182(2)	−134(1)	848(2)	38(5)
H(8B)	278(2)	−38(1)	827(2)	32(5)
H(11A)	598(2)	−147(1)	550(3)	44(6)
H(11B)	495(2)	−187(1)	404(3)	44(5)
H(12A)	628(2)	−314(1)	558(2)	34(5)
H(12B)	483(2)	−335(1)	538(2)	35(5)
H(13A)	578(2)	−249(1)	828(2)	32(5)
H(13B)	541(2)	−359(1)	831(2)	34(5)

not for absorption (μ = 7.4 cm^{-1}). Each structure factor was assigned an individual weight based on counting statistics[31].

The structure was solved with the aid of the program MULTAN '78 (ref.[32]). An E map calculated with 250 reflections (E > 1.3), having a combined figure of merit of 3.0, gave the positions of the 16 non-hydrogen atoms as the 16 highest peaks. After initial refinement with the SHELX system[33], hydrogen atoms were located in a difference map. The structure was further refined by block-diagonal least squares methods[34], with anisotropic thermal parameters for the non-hydrogen atoms and isotropic thermal parameters for the hydrogen atoms, to a final *R*-value of 0.037. Refinement was stopped when all parameter shifts were less than 25% of their standard deviation. Positional and isotropic thermal parameters for non-hydrogen atoms are given in Table II and those of hydrogen atoms in Table III (anisotropic thermal parameters for non-hydrogen atoms and structure factors are available on request (D.v.d.H.)).

The absolute configuration was determined using the Bijvoet method for the anomalous dispersion of the Cu radiation by all nitrogen, oxygen and carbon atoms in the molecule. The general procedure for the selection of the proper Friedel pairs and subsequent measurements has been detailed[35]. Briefly, this involves the repetitive measurement of the intensities for the *hkl*, *hk̄l*, *hkl̄* and *hkl̄* reflections shown to have a high sensitivity factor $\{ SF = [F^2(+) - F^2(-)]/\sigma(I)\}$. The intensities of 18 such reflections were measured 15 times at each position, then were averaged into two sets: (*hkl* and *hk̄l̄*) and (*hk̄l* and *hkl̄*). The observed and calculated values for these parameters are given in Table IV. All 18 reflections validate the absolute configuration reported, with the stereochemistry

TABLE IV

Comparison of calculated and observed Bijvoet differences DEL = $2[F^2(+) - F^2(-)]/[F^2(+) + F^2(-)] \times 100$, for the definition of SF see text

h	*k*	*l*	DEL		SF	
			obs.	calc.	obs.	calc.
11	2	3	6.44	9.07	0.63	0.28
1	3	5	6.08	4.14	2.85	0.32
6	11	3	15.86	7.82	2.31	0.26
5	4	8	−3.90	−5.13	−0.89	−0.27
3	6	2	−5.41	−5.92	−2.03	−0.45
6	6	4	3.32	3.65	1.19	0.27
3	3	8	−2.63	−3.71	−0.76	−0.25
6	8	6	6.10	4.20	1.56	0.24
8	10	3	6.33	7.74	0.77	0.23
8	11	4	5.58	5.66	1.00	0.26
5	13	1	6.61	3.77	1.37	0.25
1	15	4	4.61	9.04	0.47	0.23
3	13	4	6.28	3.39	1.53	0.24
7	11	4	−4.75	−4.35	−0.93	−0.22
1	10	5	−4.80	−2.85	−1.96	−0.22
2	7	8	3.26	3.42	0.93	0.22
3	6	1	−6.57	−2.82	−3.00	−0.22
3	3	7	−4.16	−3.72	−1.20	−0.22

of C(7) being the same as that of C(2) in (+)-(*S*)-1,2-diaminopropane. Consequently, with the relative configuration at centers C(1) and C(7) known from the classical diffraction experiment the absolute configuration at both chiral centers of *I* is established as (1*S*,7*S*).

Spectroscopic Measurements

The carbon-13 1D-NMR spectra of *I* were measured on an FT NMR spectrometer Varian XL-200 at 50.3 MHz in deuteriochloroform and referenced to tetramethylsilane using the relations $\delta(CDCl_3) = 77$ and $\delta(C_6D_6) = 128$. Proton 1D-NMR spectra, a homonuclear ^1H–^1H correlated 2D COSY spectrum[36,37] and a heteronuclear ^{13}C–^1H correlated 2D-NMR spectrum[38] were measured on a Bruker AM-400 (at 400.13 MHz and 100.6 MHz) instrument in hexadeuteriobenzene. Experimental parameters of 2D spectra are given in the corresponding figures. The simulation of spectra and simulation-iteration calculations were done using either the SPIN program (LAOCOON II: part of Varian standard software, version H1.Z) or the PANIC program (standard software of Bruker instruments).

The electronic CD spectra were determined on a Jobin Yvon Mark V Dichrographe augmented with the home-made software[39]. The measurements were performed in cyclohexane, acetonitrile, methanol, water, 2,2,2-trifluoroethanol and 1,1,1,3,3,3-hexafluoro-2-propanol (0.05–0.1 cm quartz cells, 24–26 C, concentration 1.5×10^{-3} mol l^{-1}) and as a function of temperature in methanol–ethanol (1:1, range −80 C to +40 C).

Vibrational circular dichroism (VCD) spectra were measured on a Digilab FTS-60 Fourier transform infrared spectrometer adapted at UIC for VCD measurements. The instrument and experimental procedure have been described in detail elsewhere[40]. The spectra were recorded on 0.015 M solutions in deuteriochloroform at room temperature using a variable path cell (KBr windows) set for 0.015 cm. The interferograms were scanned at 0.6 cm s^{-1} mirror velocity. The data collection involved 4 × 4096 polarization modulated interferograms and 4 × 64 transmission interferograms for both the sample and the baseline. For the baseline we utilized solvent scans, because only one enantiomer and no racemate of both compounds *I* and *II* were available. Such a measurement is possible only with our improved optical design since with very careful optical alignment there are typically no significant absorbance related artifacts (see ref.[40] for details). The VCD of the amide I band was checked on the UIC dispersive instrument[41] using a baseline simulated by obtaining a VCD spectrum of the racemic non-methylated compound for *II* and that of the 4-tert-butylhexane lactam for *I*. No significant differences were found.

RESULTS

A stereoview of the dilactam *I* in the crystalline state is shown in Fig. 1. Bond distances and angles are given in Fig. 2., ring designation and torsion angles in Fig. 3. From the sum of the bond angles about carbon atoms C(5) and C(10) and nitrogen atoms N(6) and N(9), it is clear that though the carbonyl groups are essentially planar, the bonds about the amide nitrogens vary significantly from planarity, though less so than in the case of dilactams with all of the rings being five-membered. The distortion of the amide groups is better illustrated by the conformational parameters in Table V, calculated by the convention of Winkler and Dunitz[20]. The extent of the pyramidal character of the bonds to the

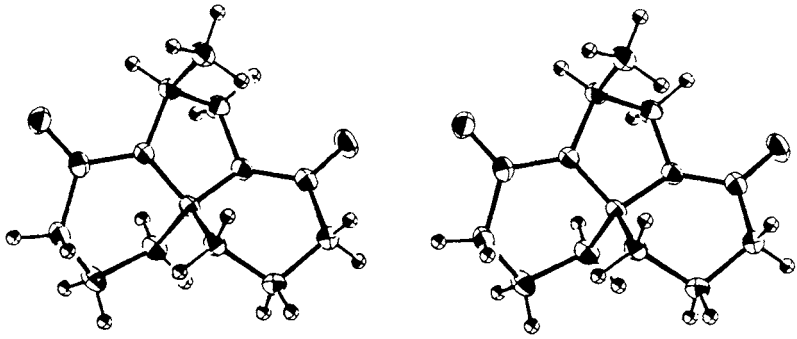

FIG. 1
Stereoview of a single molecule of *I* in the crystalline state

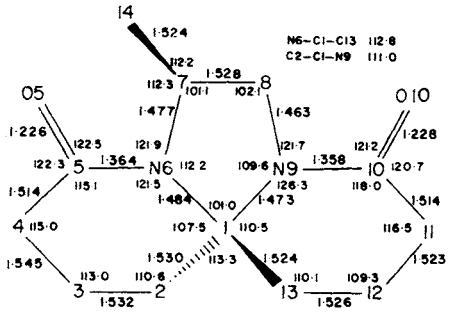

FIG. 2
Bond distances and angles of *I*. Standard deviations for bond distances are 0.002 Å; standard deviations for bond angles are 0.10–0.13°

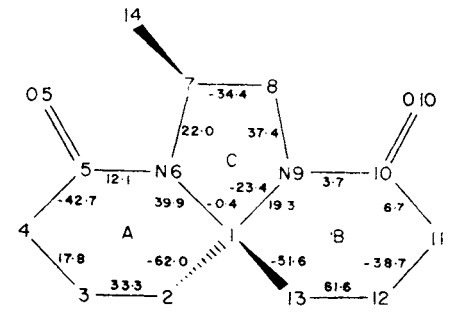

FIG. 3
Ring designation and torsion angles of *I*. Standard deviations are 0.2°

nitrogen atoms (given by the angle χ_N) is about half of the values observed in compound *III* (ref.[30]). The magnitude of this non-planar deformation is not the same for both amide groups; and, in addition, there is a significant twist of the pyramid on N in the B ring from being perpendicular to the O=C'—N plane (τ value). The geometry of this amide group is similar to the amide group within the six-membered ring of the dilactam *V* (investigated previously as a racemate[28]). The deformation of the amide bonds is reflected in a lengthening of the C—N bonds and, to lesser extent a shortening of the C=O bonds, relative to the average values for peptides (1.335 Å and 1.229 Å, respectively)[42].

Calculation of the pseudorotational parameters for rings A and B according to the method of Cremer and Pople[43] shows their conformations to be significantly different. Ring A [Q = 0.65Å, Φ_2 = 26.09°, Θ = 80.06 °] is properly described as a twist-boad conformation, but ring B [Q = 0.51Å, Φ_2 = 76.75°, Θ = 53.79°] shows a very unusual conformation, intermediate between a half-chair and half-boat. Ring B is less puckered than ring A. One result of the conformational differences between rings A and B is that the hydrogen atoms are more staggered in ring B, which is also indicated by the larger conformational angles for C(11)-C(12) and C(12)-C(13) when compared to C(3)-C(4) and C(2)-C(3) (Fig. 4). The pseudorotation parameters for ring C show the ring to be in an envelope (C_s) conformation, with C(8) at the apex (Θ = 108 as measured from C(1) to N(6) indicates C(8) as apex; Q = 0.36Å). Analysis of the packing interactions showed no unusual intermolecular contacts.

Proton decoupled ^{13}C NMR spectra in $CDCl_3$ and C_6D_6 confirmed the diastereomeric purity of *I*. Twelve observed signals correspond to the total number of carbon atoms in *I* considering the nonequivalence of carbon atoms in rings A and B. The "attached proton test" spectrum (ref.[44]) distinguished the

TABLE V
Conformational parameters for non-planar amide groups of *I* in the crystalline state (the symbols are defined according to Winkler and Dunitz[20])

Parameter	Ring A	Ring B
ω_1	166.6(2)	164.0(2)
ω_2	−170.0(2)	−174.4(2)
ω_3	−15.5(2)	−14.1(2)
ω_4	12.1(2)	3.7(2)
τ	−3.4	−10.4
χ_C	2.1	−1.9
χ_N	25.5	19.7

carbon signals according to the number of directly bonded hydrogen atoms. Together with the chemical shifts it enables us to assign unambiguously the signals of carbon atoms of the C ring (C(1,7,8 and 14)). The six CH_2 carbon atoms of A and B rings were structurally assigned with the aid of a heteronuclear ^{13}C–^{1}H correlated 2D-NMR spectrum (Fig.4) using the previously assigned ^{1}H NMR data (see below) and the coupling constants ^{1}J(C,H). The assignment of carbonyl carbon atoms is only tentative – based on the analogy with the behavior of CH_2 carbons (upfield shifts of carbon signals within ring A relative to those within the B ring). The complete ^{13}C NMR data of *I* in $CDCl_3$ and C_6D_6 are given in Table VI together with aromatic solvent induced shift (ASIS) values, one bond ^{1}H–^{13}C coupling constants and chemical shift differences of carbons in the corresponding positions of rings A and B. Significant ASIS values were found only for carbonyl carbon atoms (−1.32 and −1.20 ppm) while all other carbon atoms showed much smaller values (≦ 0.30 ppm). On the contrary, the chemical shift non-equivalence is very small for the carbonyl

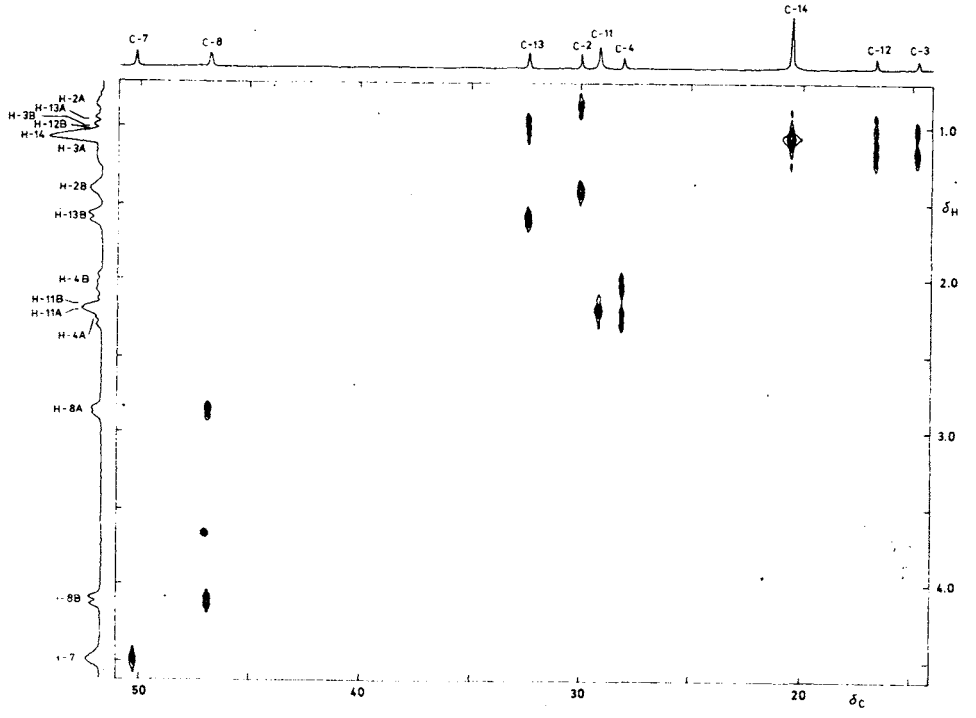

FIG. 4

^{13}C–^{1}H Heteronuclear correlated 2D-NMR spectrum of compound *I* in C_6D_6. Experimental parameters: spectral widths 3 800 Hz (^{13}C) and 810 Hz (^{1}H); 320 scans for each increment value; zero filling to data matrix 1 024 × 1 024 points

carbon atoms (< 0.32 ppm) and it increases in the order C(α) < C(β) < C(γ) in both solvents exhibiting slightly larger values in C_6D_6 (1.06 to 2.38 ppm) than in $CDCl_3$ (0.87 to 1.96 ppm). The coupling constants ^1J(C,H) allowed to distinguish the five-membered ring carbon atoms (^1J(C,H) = 146 Hz) from the six-membered and methyl carbon atoms (^1J(C,H) = 126–130 Hz). Fine splitting of signals in the proton coupled ^{13}C spectrum of I was not well resolved due to many geminal, vicinal and long-range couplings.

The ^1H NMR spectrum of *I* having eighteen protons was difficult to analyze even on a 400 MHz instrument. For the detailed analysis the spectrum in C_6D_6 was chosen because of the slightly better distribution of signals (Fig.5). The C ring protons were easier to identify because the N-CH and N-CH_2 protons give signals at the low field part of the spectrum and the methyl group appears as a strong three proton signal at 1.06 ppm. The analysis of the twelve proton spectrum of A and B rings was started with the assignment of the

TABLE VI
Carbon-13 NMR parameters of compound *I*

Carbon	Type	Chemical shift			Coupling
		in $CDCl_3$	in C_6D_6	δ(ASIS)[a]	^1J(C,H)
C(1)	>C<	76.88	76.59	−0.29	
C(2)	CH_2	30.28	30.00	−0.28	130; 130
C(3)	CH_2	14.80	14.76	−0.04	128; 128
C(4)	CH_2	27.97	28.08	0.11	130; 130
C(5)	>C=O	168.73	167.41	−1.32	
C(7)	>CH	50.12	50.15	0.03	146
C(8)	CH_2	47.02	46.80	−0.22	146
C(10)	>C=O	168.93	167.73	−1.20	
C(11)	CH_2	28.84	29.14	0.30	126; 126
C(12)	CH_2	16.56	16.63	0.07	130; 130
C(13)	CH_2	32.24	32.38	0.14	130; 130
C(14)	CH_3	20.38	20.45	0.07	128; 128; 128

Chemical shift nonequivalence

Positions	in $CDCl_3$	in C_6D_6
δ(C(13)) − δ(C(2))	1.96	2.38
δ(C(12)) − δ(C(3))	1.76	1.87
δ(C(11)) − δ(C(4))	0.87	1.06
δ(C(10)) − δ(C(5))	0.20	0.32

[a] Defined as the difference of δ(C(i)) in C_6D_6 and $CDCl_3$.

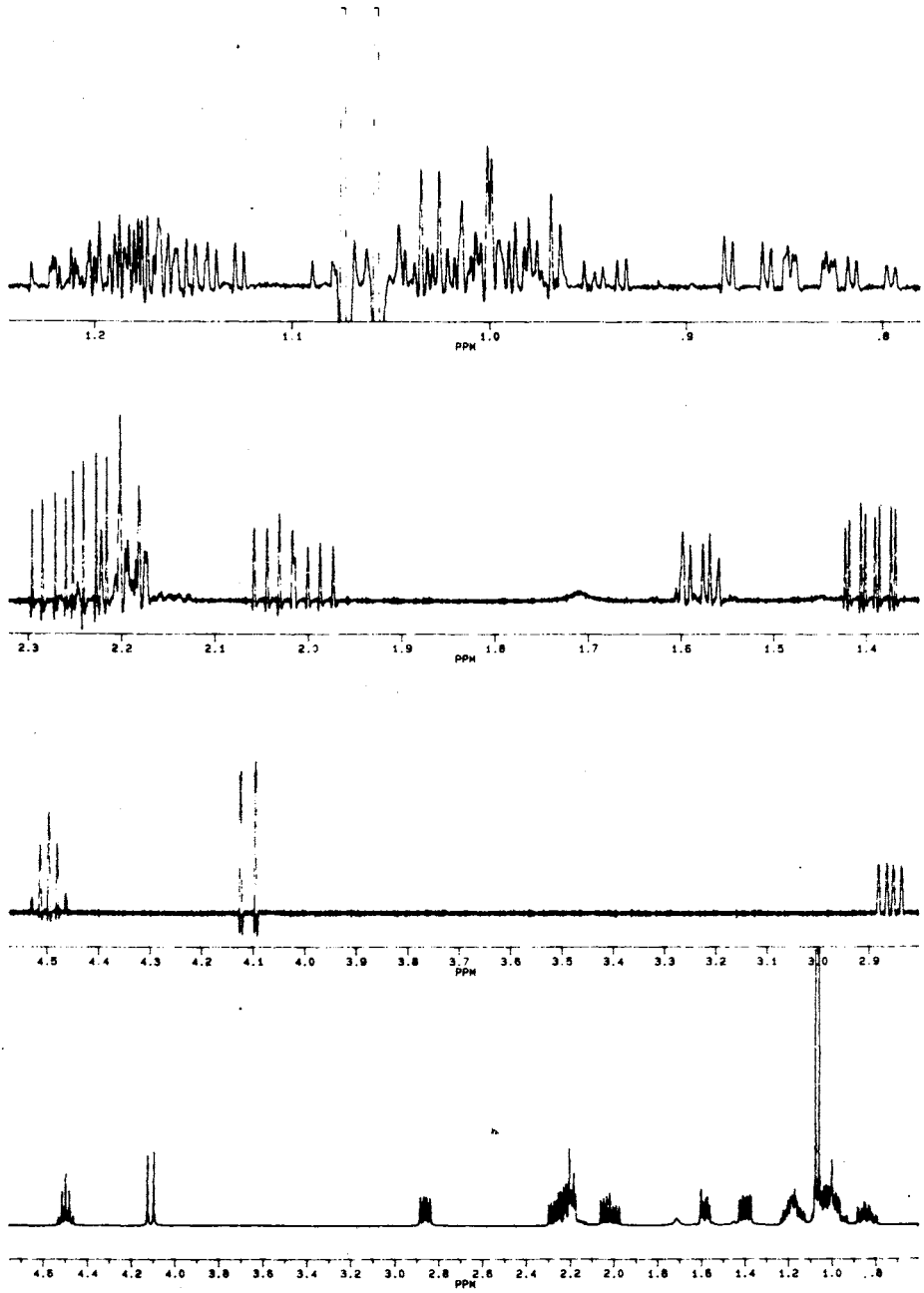

FIG. 5

Proton NMR spectrum (400 MHz) of compound *I* in C_6D_6 (below) and its expanded parts (upper traces; Gaussian apodization of FID was used for resolution enhancement)

$CO\text{-}CH_2$ signals. These were identified on the basis od their being the lowest field signals within the A,B ring system and especially on the high geminal coupling constants $^2J(H,H) \sim 18$ Hz. The mutually coupled protons of both the $\text{-}CO\text{-}CH_2\text{-}CH_2\text{-}CH_2\text{-}$ fragments were assigned with the aid of the $^1H\text{–}^1H$ 2D-COSY spectrum (Fig.6). In the next step the identified fragments were structurally assigned to the individual A, B rings. For this purpose we utilized the observed long range couplings $^5J(7,4B)$ 0.4 Hz and $^5J(8A,11B)$ 0.5 Hz. These represent a special type of homoallylic coupling where a C=C bond is substituted by a C(O)–N bond with a partial double bond character. The non-zero couplings of this type were already found in some compounds having *cis*-peptide groups (refs[45,46]). An additional long range coupling (1.8 Hz) was found between protons in the positions 2 and 13, connecting thus both A and

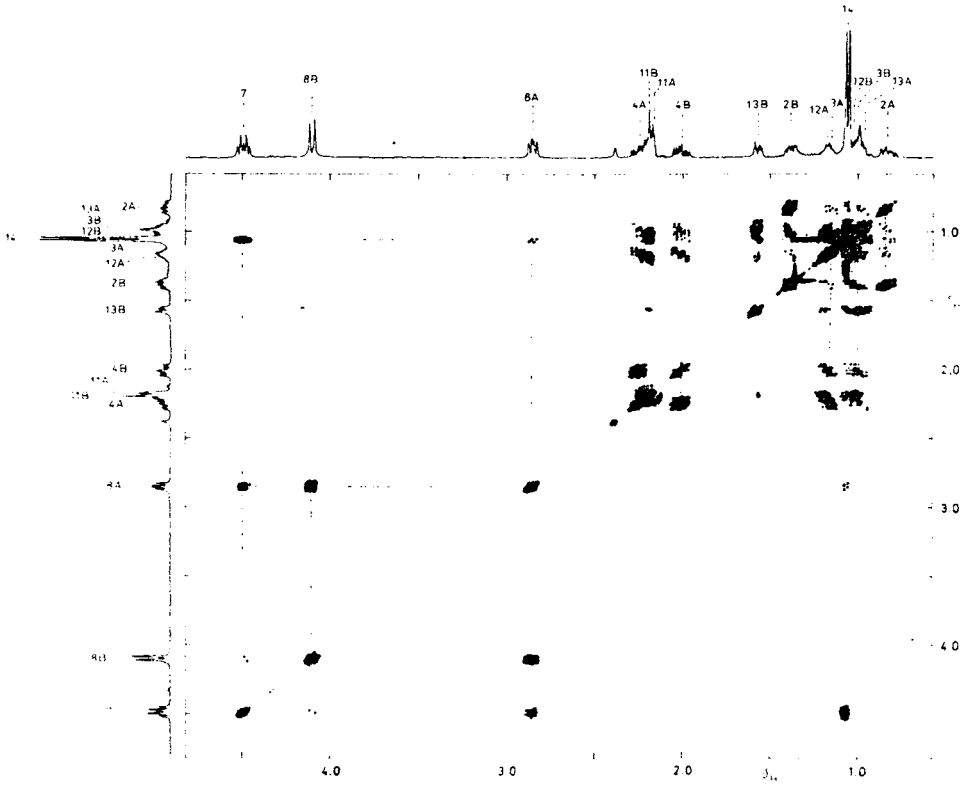

FIG. 6

Proton homonuclear correlated 2D-NMR (COSY) spectrum (400 MHz) of compound *1* in C_6D_6. Experimental parameters: spectral widths 1 700 Hz (F_2) and 850 Hz (F_1); observe pulse 45° (8.3 μs); relaxation delay 3 s; 256 increments; 32 scans for each increment value; zero filling to data matrix 4 096 × 2 048 points

B rings. As follows from molecular models, the protons H(2A) and H(13A) occupy terminal positions in a planar zig-zag arrangement of H(2A)—C(2)—C(1)—C(13)—H(13A) bonds which is the optimal arrangement for an efficient σ-coupling across four bonds. To obtain parameters for conformational analysis parameter sets obtained from the ^{1}H spectrum assigned in the above described manner were subjected to simulation-iteration calculations. Expanded parts of the 1D-NMR spectrum (where optimized resolution enhanced processing was used) afforded 1st order parameters. The calculation was executed in three parts corresponding to individual rings A,B and C. The five-membered C ring was analyzed as an $A_3BCD(M)$ spin system, where A_3BCD corresponds to protons of the $C(14)H_3$-C(7)H-$C(8)H_2$ fragment and the non-iterated spin M was included to manifest the long range coupling of H(4B) and H(11B) to H(7) and H(8A). The A ring protons were analyzed as an ABCDEF(M) spin system with ABCDEF belonging to -$C(4)H_2$-$C(3)H_2$--$C(2)H_2$- and spin M representing the long range coupling of H(13A) and H(7) to H(2A) and H(4B). For both the A and C rings all δ and J values were obtained with high accuracy (rms 0.059 and 0.037 Hz). The spin system of the B ring was most difficult to analyze, because strongly coupled and partially overlapping signals bring serious complications. The resulting parameter set, obtained again from the analysis of the ABCDEF(M) spin system (with the spin M manifesting the long range coupling of H(8A) and H(13A) protons), is not therefore as accurate as the two preceding cases (rms 0.3 Hz). The complete list of calculated ^{1}H NMR parameters is given in Table VII.

The observed extreme values of some ^3J(H,H) constants, the non-zero long range couplings and the independence of electronic CD spectrum of *I* on temperature (see below) provide some evidence on the rigidity of the compound and on the existence of one dominating conformer in solution. To determine the preferred conformation we utilized a relation of experimental vicinal coupling constants ^3J(exp) (Table VII) to the torsion angle Φ of interacting protons. We have chosen the empirically generalized Karplus equation (*1*)

$$^3J(H,H) = P_1\cos^2\Phi + P_2\cos\Phi + P_3 + \Sigma\Delta\chi_i\{P_4 + P_5\cos^2\Phi[\xi_i\Phi + P_6(\Delta\chi_i)]\} \quad (1)$$

including the substituent electronegativity effects as described by Haasnot et al.[47] for di- or trisubstituted ethane fragments. The torsion angle Φ is defined in the same way as in the X-ray data, ξ_i adopts two allowed values +1 or −1 (depending on the relative orientation of the given proton and the substituent — see ref.[47]) and the electronegativity term $\Delta\chi_i$ is calculated as $\Delta\chi_i = \Delta\chi_i(\alpha$ subst.) $- P_7\Sigma\Delta\chi_i(\beta$ subst.) using Huggins electronegativities for substituents in α- and β-positions[48]. With the parameter set given as a footnote to Table VIII

we have calculated the theoretical coupling constants J(calc) for the Φ angles found by X-ray analysis. Their comparison with the J(exp) values showed a very good agreement for the five-membered C ring but more significant differences were found for both the six-membered A and B rings. To estimate these conformational differences we calculated torsion angles from J(exp) values (using the graphical method and a small computer program for calculating the $J = f(\Phi)$ plots). This procedure results, for each J(exp) in one or two pairs of values which differ in sign of the Φ angle. The inspection of molecular models enables us to estimate ranges of the theoretically possible values and, consequently, usually eliminates one half of the calculated data. Further limitation follows from the inter-relations between the four torsion angles

TABLE VII
Proton NMR parameters of compound *I* in C_6D_6

Proton	δ(H(i))	J(H(i),H(j))
		Ring A
H-2A	0.837	J(2A,2B) −13.27; J(2A,3A) 7.85; J(2A,3B) 12.52; J(2A,13A) 1.80
H-2B	1.392	J(2B,2A) −13.27; J(2B,3A) 1.83; J(2B,3B) 7.15
H-3A	1.168	J(3A,3B) −14.09; J(3A,2A) 7.85; J(3A,4A) 10.02; J(3A,4B) 5.53
H-3B	1.011	J(3B,3A) −14.09; J(3B,2A) 12.52; J(3B,2B) 7.15; J(3B,4A) 4.36; J(3B,4B) 10.98
H-4A	2.250	J(4A,4B) −17.45; J(4A,3A) 10.02; J(4A,3B) 4.36
H-4B	2.014	J(4B,4A) −17.45; J(4B,3A) 5.53; J(4B,3B) 10.98; J(4B,7) 0.36
		Ring B
H-11A	2.21	J(11A,11B) −18.2; J(11A,12A) 8.1; J(11A,12B) 8.7
H-11B	2.17	J(11B,11A) −18.2; J(11B,12A) 2.7; J(11B,12B) 8.7; J(11B,13B) 1.0; J(11B,8A) 0.5
H-12A	1.19	J(12A,12B) −14.0; J(12A,11A) 8.1; J(12A,11B) 2.7; J(12A,13A) 4.9; J(12A,13B) 4.3
H-12B	1.03	J(12B,12A) −14.0; J(12B,11A) 8.7; J(12B,11B) 8.7; J(12B,13A) 13.4; J(12B,13B) 4.4
H-13A	0.97	J(13A,13B) −13.3; J(13A,12A) 4.9; J(13A,12B) 13.4; J(13A,2A) 1.8
H-13B	1.58	J(13B,13A) −13.3; J(13B,12A) 4.3; J(13B,12B) 4.4
		Ring C
H-7	4.493	J(7,8A) 6.47; J(7,8B) 0.73; J(7,14) 6.70; J(7,4B) 0.36
H-8A	2.856	J(8A,8B) −11.56; J(8A,7) 6.47; J(8A,11B) 0.51; J(8A,14) 0.54
H-8B	4.106	J(8B,8A) −11.56; J(8B,7) 0.73
H-14	1.063	J(14,7) 6.70; J(14,8A) 0.54

TABLE VIII

Comparison of interproton torsion angles Φ for *I* in crystal (X-ray) and solution (^{1}H NMR). Crystallographically determined parameters affecting the ^2J(H,H) and ^3J(H,H) together with theoretical and experimental values of these constants are given

Fragment	X-ray [a]						^{1}H NMR		
	d_1	d_2	d_3	α_1	α_2	Φ (exp.)	J (calc.)[b]	J (exp.)	Φ (exp.)[c]
Ring A									
H(2A)-C(2)-H(2B)	1.02	–	1.00	108.1	–	–	–	−13.27	–
H(3A)-C(3)-H(3B)	0.98	–	0.97	102.5	–	–	–	−14.09	–
H(4A)-C(4)-H(4B)	0.96	–	0.94	104.1	–	–	–	−7.45	–
H(2A)-C(2)-C(3)-H(3A)	1.02	1.532	0.98	109.3	107.3	37.1	7.93	7.85	39
H(2A)-C(2)-C(3)-H(3B)	1.02	1.532	0.97	109.3	108.8	147.4	10.49	12.52	155
H(2B)-C(2)-C(3)-H(3A)	1.00	1.532	0.98	110.8	107.3	−82.0	0.29	1.83	−74
H(2B)-C(2)-C(3)-H(3B)	1.00	1.532	0.97	110.8	108.8	28.3	9.53	7.15	42
H(3A)-C(3)-C(4)-H(4A)	0.98	1.545	0.96	111.3	111.4	20.1	10.90	10.02	12
H(3A)-C(3)-C(4)-H(4B)	0.98	1.545	0.94	111.3	109.8	134.8	7.53	5.53	133
H(3B)-C(3)-C(4)-H(4A)	0.97	1.545	0.96	113.3	111.4	−94.9	0.39	4.36	−113
H(3B)-C(3)-C(4)-H(4B)	0.97	1.545	0.94	113.3	109.8	19.9	11.05	10.98	8
Ring B									
H(13A)-C(13)-H(13B)	0.92	–	0.97	107.5	–	–	–	−13.3	–
H(12A)-C(12)-H(12B)	1.02	–	0.94	106.6	–	–	–	−14.0	–
H(11A)-C(11)-H(11B)	1.02	–	1.00	112.3	–	–	–	−18.2	–
H(13A)-C(13)-C(12)-H(12A)	0.92	1.526	1.02	107.6	111.4	63.3	2.50	4.9	54
H(13A)-C(13)-C(12)-H(12B)	0.92	1.526	0.94	107.6	110.5	−178.4	14.42	13.4	166
H(13B)-C(13)-C(12)-H(12A)	0.97	1.526	1.02	112.5	111.4	−54.8	3.96	4.3	−56
H(13B)-C(13)-C(12)-H(12B)	0.97	1.526	0.94	112.5	110.5	63.4	2.33	4.4	56
H(12A)-C(12)-C(11)-H(11A)	1.02	1.523	1.02	109.8	106.6	−42.6	6.74	8.1	−37
H(12A)-C(12)-C(11)-H(11B)	1.02	1.523	1.00	109.8	110.5	79.7	0.41	2.7	74
H(12B)-C(12)-C(11)-H(11A)	0.94	1.523	1.02	109.2	106.6	−159.1	12.72	8.7	−147
H(12B)-C(12)-C(11)-H(11B)	0.94	1.523	1.00	109.2	110.5	−36.8	7.82	8.7	−38
Ring C									
H(8A)-C(8)-H(8B)	1.01	–	1.01	109.4	–	–	–	−11.55	–
H(8A)-C(8)-C(7)-H(7)	1.01	1.528	0.97	113.7	115.6	−31.9	6.30	6.47	−35
H(8B)-C(8)-C(7)-H(7)	1.01	1.528	0.97	112.2	115.6	92.8	1.53	0.73	80

[a] Standard deviations of C–H bond lengths are 0.02 Å; of bond angles involving one H atom are 0.9–1.2°; of bond angles involving two H atoms are 1.4–1.7°; and of torsion angles involving two H atoms are 1.4–1.8°; [b] *J*-values calculated from Eq. (*1*); for protons of A and B rings with parameters: $P_1 = 13.89$, $P_2 = -0.98$, $P_3 = 0$, $P_4 = 1.02$, $P_5 = -3.40$, $P_6 = 14.9°$, $P_7 = 0.24$; for C ring protons: $P_1 = 13.70$, $P_2 = -0.73$, $P_3 = 0$, $P_4 = 0.56$, $P_5 = -2.47$, $P_6 = 16.9°$, $P_7 = 0.14$; [c] Φ-values calculated from Eq. (*1*) with parameters given in footnote *b* and modified to fit conditions discussed in text.

within each $-CH_2-CH_2-$ fragment of the A and B rings: (i) absolute value of the largest torsion angle must be equal to a sum of absolute values of the remaining three torsion angles; (ii) the sum of absolute values of the two torsion angles Φ of a CH_2 group with any neighbouring proton is equal to a projection of the CH_2 valence angle α with limited values (in our case the range 110 ° to 125 ° was chosen in accord with X-ray results). Application of the above criteria allowed us to find one set of Φ values for each $-CH_2-CH_2-$ fragment. A slight modification of Φ values provided a final set which fits the above numerical conditions together with the minimum differences between J(calc) and J(exp) values (rms 0.93 Hz). These Φ(calc) values are given in Table VIII. They indicate that the preferred solution conformation of the compound *I* is very similar to the crystal structure. The mean deviation of Φ's for crystal and solution is 8 °. It is evident that the calculated Φ values for the solution conformation are less accurate than crystal structure data. However it is difficult to estimate errors arising from the Karplus equation used and/or from a non-negligible population of another conformer in solution. One must therefore be careful in interpreting small differences in Φ values as an indication of a different solution conformation.

Electronic CD spectra of *I* (Table IX, Fig.7) display a positive band with the maximum position shifting to the blue from 220 nm to 211 nm with increasing solvent polarity. Simultaneously its intensity increases by about a factor of two. In the short wavelength region (185 – 200 nm) there is a negative dichroic band of lower intensity. Its maximum is discernible only in fluorinated alcohols, in other solvents only a negative tail is detected. In the less polar solvents, cyclohexane and acetonitrile, there is a shoulder between the two bands (at about 200 nm). This basically two-band pattern is very similar to that found for the previously investigated monolactams derived from the twistane skeleton[12-17]. In these molecules the observed electronic optical activity is supposed to arise mainly from the inherent chirality of the non-planar amide chromophore. On the other hand, a comparison with spectra of closely related dilactams *II* – *IV* (ref.[30]) (considering the same absolute configuration) reveals significant differences concerning the band pattern and the intensity. The spectra of *II* – *IV* show a well developed exciton like couplet in the π–π^* transition region. There is a positive π–π_1^* peak of high intensity ($[\Theta]_{max} \sim 5.10^4$) at about 205 nm and a negative tail towards higher energies which obviously belongs to the second (π–π_2^*) component. The position and intensity of the positive band is almost insensitive to solvent and temperature changes. The n–π^* band at the low energy side of the π–π_1^* peak is also positive, smaller ($[\Theta]_{max} \sim 2-3.10^4$) but large enough to be manifested as a partially separated band in less polar solvents and as a distinct shoulder in fluorinated alcohols. With *I* the situation is different. There is only one positive band above 200 nm and a shoulder, if any,

is observed at its high energy side. The intensity of the positive band corresponds approximately to the n–π^* band of *II* or *III* in non-polar solvents and its position is about in the middle of what is expected for the n–π^* and $\pi - \pi_1^*$ bands. The band is quite wide and its solvent induced shifts are smaller than for *II* – *IV*. Hence it seems probable that the positive CD band of *I* results from overlap between the two positive (n– π^* and π–π_1^*) components. This assignment is further supported by the fact that the negative band beyond 200 nm is too high in energy to be a sole manifestation of π–π^* transitions in a molecule containing

TABLE IX
Electronic CD spectra of the spirodilactam *I*. Wavelengths of apparent maxima in nm, $[\Theta]$ ($\times 10^{-3}$) values in parentheses

Solvent[a]	n–π^* region	π–π^* region
Cyclohexane	220(25.1)	195 s, 185 n
Acetonitrile	217(34.7)	195 s, 185 n
Methanol	214(47.2)	190 n
Water	212(53.5)	192 s, 185 n
TFE	212(49.8)	188(−15.5)
HFP	211(54.7)	187(−22.5)
Methanol–ethanol (+40°C)	215(54.1)	[b]
Methanol–ethanol (−80°C)	214(66.3)	[b]

[a] Measured at room temperature unless otherwise stated; [b] not measured; s shoulder; n negative CD but without a maximum.

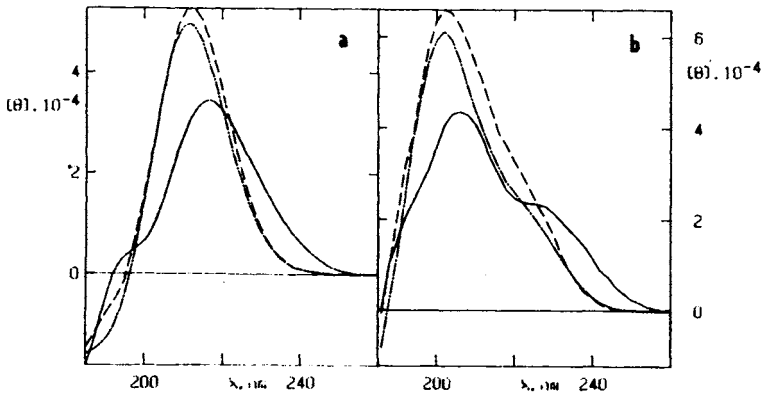

FIG. 7
Electronic circular dichroism of the dilactams *I* (a) and *II* (b). Solutions in acetonitrile (———), water (– – – –), TFE (– · – · –)

tertiary amide groups. Thus it seems that the general sign pattern of CD bands is the same as in *II*–*IV*. The n–π^* band approximately retains its magnitude, but the intensity of the π–π^* couplet is much smaller (estimated as about 30 %, at most) precluding direct observation of the π–π_1^* component. The shoulder at 200 nm might be a direct evidence of the presence of this component, but other explanations cannot be excluded (intermolecular association or a Rydberg type transition, see e.g.[12,13]). Another support for the existence of the positive π–π_1^* component might be the intensity increase of the positive band in polar solvents (provided that under these conditions the exciton couplet gains more intensity). Evidently, the spectra of *I* are seriously influenced by superposition of closely lying bands. For this reason we do not report experimental rotational strengths. The variation of temperature had no appreciable effect. The compound appears to be rigid, at least in alcohols.

In Fig. 8 FTIR VCD and absorption spectra are given of *I* and *II* in the amide I and mid-ir region. Both spirodilactams exhibit monosignate negative amide I VCD of moderate intensity with the peak positions corresponding to the absorption maxima (1 635 cm^{-1} for *I*, 1 693 cm^{-1} for *II*) and *I* weaker than *II*. This difference of amide I band positions for *I* and *II* has been noted previously[1,2] and correlated to the effects of different bond angles on carbonyl C atom within five- or six-membered rings and of the different non-planarities of the amide groups. In the mid-ir region (1 400 – 1 000 cm^{-1}) there are several

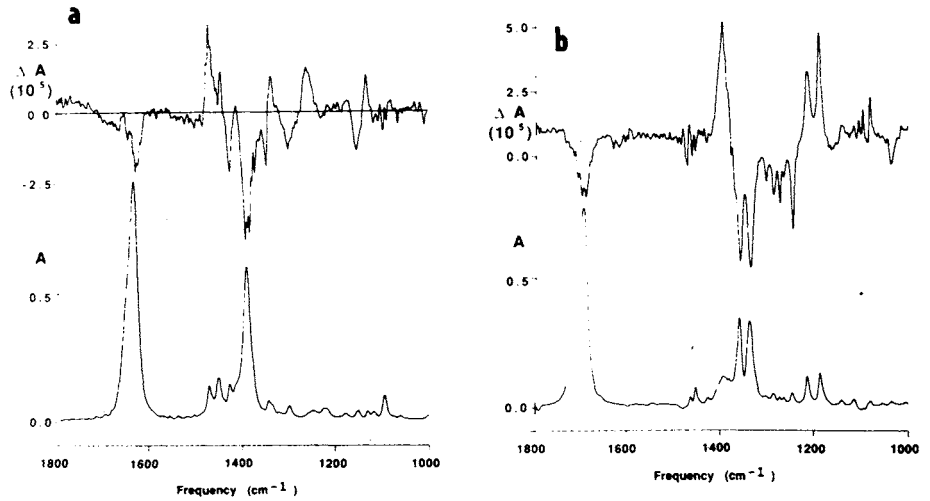

FIG. 8
VCD and absorption spectra of *I* (a) and *II* (b) in the amide I and mid-ir region

discernible VCD bands. A clear difference is present between the patterns seen in both molecules. VCD of the dilactam *II* is stronger and the particular features are much better resolved. There are two strong VCD patterns composed of a sequence of three bands with the highest energy peak of one sign, the other two of the other (Fig. 8*a*). The first set is centered around 1 360 cm^{-1} (1 397, 1 360, 1 338), the second around 1 220 cm^{-1} (1 250, 1 218, 1 190). The large VCD at 1 360 cm^{-1} correlates to expected C—N stretching motion (analogous to the Amide III). The pattern seen is reminiscent of that expected for a coupled oscillator and correlates with the most intense mid-ir absorptions. The lower frequency intense VCD pattern ($\sim$ 1 220 cm^{-1}) is not possible to assign so simply. The VCD of *I* is less intense and generally lacks leading features. The spectrum is not dominated by a few bands, but a series of intermediate intensity bands is found over a much wider region. The C—N stretches (intense absorptions at $\sim$ 1 400 cm^{-1}) are shifted to higher energy and have VCD complicated by overlap with the CH deformation modes. The CH_2 scissor motions ($\sim$ 1 450 cm^{-1}) have little VCD in the five-membered ring system (*II*) but have substantial VCD in the six-membered (*I*). With the exception of the 1 357 cm^{-1} peak of *I*, all the above mentioned VCD bands correspond to absorption maxima.

DISCUSSION

X-Ray analysis of the compound *I* confirmed the expected less non-planar amide groups in the tricyclic system containing six-membered lactam rings. When these data are compared to other spirocyclic dilactams (Table X) it is possible to find out the following more general features: (i) For these systems χ_N and τ are interrelated by an approximate relation $-2\tau \sim \chi_N$ (the two angles are

TABLE X
Non-planarity parameters of amide groups in spirodilactams

Compound	χ_N	χ_C	τ
I (ring A)[a]	25.5	2.1	−3.4
I (ring B)[a]	19.7	−1.9	−10.4
III (ring A)[b]	42.1	0.0	−26.7
III (ring B)[b]	39.5	−0.3	8.6
IV[c]	−42.0	−0.3	21.3
V (5-membered ring)[d]	−41.2	0.0	20.8
V (6-membered ring)[d]	−16.7	0.9	17.8
VI[e]	−43.7	−0.2	20.5
VII[e]	−19.1	−0.6	7.3

[a] This paper, see Table V; [b] ref. [30]; [c] ref. [26]; [d] ref. [28]; [e] ref. [27].

always of opposite signs), the biggest exception being the ring A of the compound *I*. In this case τ is small and the amide deformation is a nearly pure pyramid on N. Another exception is a compound *V* (with one lactam ring five-membered, the other one six-membered) exhibiting unusually big τ for the six-membered ring. (ii) The values of χ_C are close to zero in the whole series of these compounds (and, in fact, in all model lactams investigated so far), yet these values are somewhat larger for the six-membered rings. (iii) For compounds lacking rotational symmetry the non-planar deformation is not equally divided between the two lactam rings, even if they are of the same size (see compound *III*). In general, the above statements indicate that even in these rather rigid polycyclic systems only approximate predictions can be made about the main (χ_N and τ) non-planarity parameters.

The detailed NMR study of *I* was aimed to check whether molecular geometry found in the crystal is transferable to the compound in solution. In general, the structure appears transferable. NMR data do not indicate any major conformational change, however the observed minor variations of dihedral angles do not exclude small changes within the same conformational type. Unfortunately NMR data do not provide detailed information about amide group geometry, in this respect they are merely limited to distinguishing *cis*- and *trans*-amide bonds. In principle, such parameters as $\delta(^{13}C)$ of C=O, $\delta(^{15}N)$, $\delta(^{17}O)$ of C=O and $^1J(^{15}N,^{13}C)$ and with amides also $^1J(^{15}N,^1H)$ or $^3J(^{13}C\text{-}CO\text{-}N\text{-}H)$ could be useful for obtainig direct data about the amide group distortion. But experimental difficulties with obtaining most of these NMR parameters and/or their unclear relation to amide geometry seriously limit this attempt. It seems necessary to collect much more NMR studies on proper model compounds till the geometry of the amide group will be accessible from NMR data.

The fact that the observed electronic circular dichroism resembles that of mono-lactams with non-planar amide groups suggests that the decisive source of optical activity in this compound is again the inherent chirality of non-planar amides. At first glance this observation appears surprising, because the much more structurally related dilactams *II*–*IV* having moreover bigger non-planar deformations exhibit CD spectra dominated in the π–π^* region by the exciton-like couplet. Considered in general, the electronic circular dichroism of *I* (positive in the region of the n–π^* transition, negative below 195 nm) is, for the given absolute configuration, in agreement with the rule proposed for the inherent chirality of non-planar amide group (tertiary amide treated as a transoid case, $\chi_N > 0$, τ neglected). The neglect of the twist parameter τ means that we are using an amide bond distorted by a pure pyramid on N for this comparison. This assumption is better justified for *I* when compared to compounds *II*–*IV* since for *I* τ is small within the A ring. Optical activity

calculations predict a different CD pattern for an amide distorted by torsion[8] (both n–π^* and π–π^* bands are calculated to be of the same sign, i.e. a cancellation in one of the regions is indicated when both pyramidal and torsional deformations are present in combination). Considering this structural difference between *I* and *II*–*IV* it seems a reasonable explanation that for *I* the observed CD is determined by the amide chirality due to the more purely pyramidal amide nitrogen in the A ring, while for *II*–*IV* the non-planarity effects are suppressed in the π–π^* region due to the twist. On the other hand, especially the band positions of *I* cannot be explained on the basis of such a simple interpretation. The exciton contribution, though not directly observed, is still present in the spectra of *I*. Its low magnitude should be connected either with mutual orientation of amide groups in five- or six-membered rings A and B or with a change of transition dipole orientation within amide groups when these are distorted. As can be derived from X-ray data, the size of the lactam rings significantly affects the angle between the two planes containing O=C'—N atoms (35° for *I* and 52° for *III*). We have tried to calculate coupled oscillator contribution to optical activity of *I* and *III* using X-ray geometries, absorption data of the tertiary amide derived from twistane[49] and transition dipole orientation as given by Woody[50] for planar amides. The results were in a reasonable agreement with the CD of *III* (proper signs of the π–π^* couplet, $[R] = 3 \cdot 38.10^{-39}$ esu^{2}cm^2, band splitting 10.2 nm), but almost the same values were calculated for the geometry of *I* ($[R] = 3 \cdot 44.10^{-39}$ esu^{2}cm^2, band splitting 10.7 nm). It seems probable that changes of transition dipole orientations should include non-planarity effects, however this requires a much more detailed computational study. At present, these calculations do not explain the small magnitude of the π–π^* couplet in the spectra of *I*. Alternatively, the CD can originate in the ring chirality. Unfortunately such an effect cannot be evaluated since the influence of a chiral environment on non-planar amides is not known. In summary, the electronic CD of *I* is clearly correlated with the amide group non-planarity, however several details of the spectra remain to be explained.

VCD spectra in Fig. 6 represent the first successful measurements on compounds with non-planar amide groups in a rigid environment. It might be expected that these two molecules would behave as coupled oscillators, particularly for the intense bands. However the two C=O stretches, due to their nearly colinear orientation, have a very small coupled oscillator VCD. Indeed we see only single-signed VCD for this band. It might arise from some phenomenon like ring currents as modelled by Nafie and Freedman[51]. However, the fact that we have failed to identify any such VCD in several other polycyclic mono-lactams[52], with and without non-planar amide groups, argues against the observed VCD of *I* and *II* having arisen from such a local phenomenon.

Alternatively, single-signed VCD can arise through coupling of all the normal modes which would have a difficult-to-discern dependence on the amide non-planarity. One possible factor is that the conformation of amide groups affects the overall VCD amplitude. In an effort to explore this question further, we have undertaken a series of empirical VCD (fixed partial charge – FPC) calculations[53] for both *I* and *II*. To carry out these preliminary tests a force field is required. With such large molecules, only an approximate force field is possible, so we chose to use the Warshel–Lifson consistent force field[54] as a starting point. In previous studies[55], this has yielded useful pictures of the C—H stretching VCD of smaller molecules but application to the mid-ir on such a large molecule has never been attempted. The diagonal force constants were modified slightly to give reasonable frequencies for selected modes. The geometries from the crystal structure results were used for comparative purposes. In both cases these corresponded reasonably well to the minimum energy structures found via the optimization routine. For *II* we tried 8 different starting conformers and the lowest energy structure was similar to that in the X-ray report[26]. However, several other minima were found within a range of 8 kJ/mol. For *I* there were too many possibilities for an inclusive test, so we searched for the likely minima using a dynamics calculation running at 10 000 K with CHARMM (ref.[56]). No conformers more stable than that corresponding to the crystal structure were found.

Preliminary FPC results were very encouraging for the compound *II* (five-membered rings). A negative VCD was calculated for the C=O stretch, while, virtually no VCD was calculated for the CH_2 scissors and a strong VCD couplet of the correct sense and magnitude (in terms of $\Delta\varepsilon/\varepsilon$) was calculated for the C—N stretches. The overall magnitudes, as is typical of FPC calculations, were low compared to the experimental results. In particular, $\Delta\varepsilon/\varepsilon$ for the Amide I, C=O, stretch was ten times too small, however the C—N results were comparable to what was measured. Nothing in the calculation fit the large VCD at $\sim$ 1 220 cm^{-1} even in a qualitative sense. In the compound *I* (six-membered rings), virtually no such detailed alignment of calculation and experiment was possible. The only reliable indication was that the C=O stretch was again small (but of the wrong sign) and now significant VCD intensity was calculated for the CH_2 scissors as well as the C—N stretches in the mid-ir. The FPC type calculations fundamentally reflect possible dipolar coupling under the limitations imposed by the very severe approximations implicit in the model. The lack of intensity in the C=O stretch as compared to the mid-ir indicates that its VCD must arise from other mechanisms. From the comments above regarding the ring current possibilities, it appears that a complex mechanism may be needed to explain these data. The C—N and CH_2 scissor motions may be usefully modelled with a dipolar coupling model, but the size of these

molecules prohibits a reliable determination of the normal modes under consideration and thus of the orientation of the dipoles being coupled. We did evaluate the coupling of the C=O modes and found that $\Delta\varepsilon/\varepsilon < 2.10^{-6}$ which would not be detectable in the presence of the single-signed band observed.

Simpler to describe modes can be found in the C–H stretching region of the spectrum. For our compounds, however, their near degeneracy and large number make detailed calculation difficult. It is interesting to note that the observed sign pattern in the VCD of the C–H stretches of *I* (not shown here) closely mimics that seen in (+)-3-methylcyclohexanone[55,52] and that in *II* has the same overall sense as in (+)-3-methylcyclopentanone[57]. In the former case, such a correlation has been attributed to coupling of CH_2 asymmetric stretches in the ring[58]. If this correlation holds ring B in the half chair conformation would be expected to dominate the C–H stretching VCD as ring A in the boat conformation would have minimal coupling between CH_2 groups.

In summary, while the overall intensity of the VCD was experimentally found to correlate with amide group non-planarity, the mechanism is unclear, at present. In fact, the details of the mid-ir data, in particular, have no obvious correlation to the amide conformation. However this overall effect, in some sense even reflected in the crude FPC calculation, may prove useful in subsequent studies of non-planar lactams or other strained systems.

CONCLUSIONS

We have shown that a combined use of X-ray diffraction, NMR spectroscopy and circular dichroism, both electronic and vibrational, is capable of providing a rather deep insight into details of molecular conformation such as the non-planarity of the amide group. This paper demonstrates the importance of special tailor-made model compounds for such studies. However even with these rigid models not all interesting questions have been answered. There is still a need to get a better theoretical understanding of electronic CD and to collect more VCD spectra on similar models (possibly using deuterated derivatives). Work along these lines is in progress.

The work at the University of Illinois at Chicago was supported by a grant from the National Institutes of Health (GM 30147) *for which we are most grateful. The* FTIR *was in part funded by the National Science Foundation* (CHE 85-11753). *The work at the University of Oklahoma was supported by* NIH *grant* GM 21822. *We wish to thank Prof. R. Elber for help with the* CHARMM *calculations.*

REFERENCES

1. Smolíková J., Bláha K.: Chem. Listy *69*, 1009 (1975).
2. Bláha K., Maloň P.: Acta Univ. Palacki. Olomuc. *93*, 81 (1980).

3. Ramachandran G.N., Kolaskar A.S.: Biochim. Biophys. Acta *303*, 385 (1973).
4. Costain C.C., Dowling J.M.: J. Chem. Phys. *32*, 158 (1960).
5. Hirota E., Sugisaki R., Nielsen C.J., Sorensen G.O.: J. Mol. Spectrosc. *49*, 251 (1974).
6. Ramachandran G.N., Lakshminarayanan A.V., Kolaskar A.S.: Biochim. Biophys. Acta *303*, 8 (1973).
7. Kolaskar A.S., Lakshminarayanan A.V., Sarathy K.P., Sasisekharan V.: Biopolymers *14*, 1081 (1975).
8. Maloň P., Bystrický S., Bláha K.: Collect. Czech. Chem. Commun. *43*, 781 (1978).
9. Tvaroška I., Bystrický S., Maloň P., Bláha K.: Collect. Czech. Chem. Commun. *47*, 17 (1982).
10. Christensen D.H., Kortzeborn R.N., Bak B., Led J.J.: J. Chem. Phys. *53*, 3912 (1970).
11. Dunitz J.D., Winkler F.K.: Acta Crystallogr., B *31*, 251 (1975).
12. Tichý M., Dušková E., Bláha K.: Tetrahedron Lett. *1974*, 237.
13. Frič I., Maloň P., Tichý M., Bláha K.: Collect. Czech. Chem. Commun. *42*, 678 (1977).
14. Maloň P., Bláha K.: Collect. Czech. Chem. Commun. *42*, 687 (1977).
15. Smolíková J., Tichý M., Bláha K.: Collect. Czech. Chem. Commun. *41*, 413 (1976).
16. Bláha K., Maloň P., Tichý M., Frič I., Usha R., Ramakumar S., Venkatesan K.: Collect. Czech. Chem. Commun. *43*, 3241 (1978).
17. Tichý M., Maloň P., Frič I., Bláha K.: Collect. Czech. Chem. Commun. *44*, 2653 (1979).
18. Klyne W., Kirk D.N., Tilley J., Suginome H.: Tetrahedron *36*, 543 (1980).
19. Boyd D.B., Riehl J.P., Richardson F.S.: Tetrahedron *35*, 1499 (1979).
20. Winkler F.K., Dunitz J.D.: J. Mol. Biol. *59*, 169 (1971).
21. Woody R.W.: Biopolymers *22*, 189 (1983).
22. Pančoška P., Frič I., Bláha K.: Collect. Czech. Chem. Commun. *44*, 1296 (1979).
23. Vičar J., Maloň P., Trka A., Smolíková J., Frič I., Bláha K.: Collect. Czech. Chem. Commun. *42*, 2701 (1977).
24. Bláha K., Farag A.M., van der Helm D., Hossain M.B., Buděšínský M., Maloň P., Smolíková J., Tichý M.: Collect. Czech. Chem. Commun. *49*, 712 (1984).
25. Smolíková J., Koblicová Z., Bláha K.: Collect. Czech. Chem. Commun. *38*, 532 (1973).
26. Ealick S.E., van der Helm D.: Acta Crystallogr., B *31*, 2676 (1975).
27. Ealick S.E., Washecheck D.M., van der Helm D.: Acta Crystallogr., B *32*, 895 (1976).
28. Ealick S.E., van der Helm D.: Acta Crystallogr., B *33*, 76 (1977).
29. Bláha K., Buděšínský M., Frič I., Koblicová Z., Maloň P., Tichý M.: Tetrahedron Lett. *1978*, 3949.
30. Bláha K., Buděšínský M., Koblicová Z., Maloň P., Tichý M., Baker J.R., Hossain M.B., van der Helm D.: Collect. Czech. Chem. Commun. *47*, 1000 (1982).
31. van der Helm D., Ealick S.E., Burks J.E.: Acta Crystallogr., B *31*, 1013 (1975).
32. Main P., Hull S.E., Lessinger L., Germain G., Declercq J.P., Woolfson M.M.: *Multan 78. A System of Computer Programs for the Automatic Solution of Crystal Structures from X-ray Diffraction Data.* Univs. of York, England and Louvain-La-Neuve, Belgium 1978.
33. Sheldrick G.M.: Shelx-76. University Chemical Laboratory, England, 1976.
34. Ahmed F.R.: SFLS *Program NRC-10*. Ottawa, National Research Council, 1966.
35. Ealick S.E., van der Helm D., Weinheimer A.J.: Acta Crystallogr., B *31*, 1618 (1975).
36. Aue W.P., Bartholdi E., Ernst R.R.: J. Chem. Phys. *64*, 2229 (1976).
37. Nagayama K., Kumar A., Wüthrich K., Ernst R.R.: J. Magn. Reson. *40*, 321 (1980).
38. Bax A., Morris G.: J. Magn. Reson. *42*, 501 (1981).
39. Maloň P.: *Dichrosoft Program*. Inst. Org. Chem. Biochem., Prague 1984.
40. Maloň P., Keiderling T.A.: Appl. Spectrosc. *42*, 32 (1988).
41. Keiderling T.A.: Appl. Spectrosc. Rev. *17*, 189 (1981).

42. Karle I.L. in: *The Peptides* (E. Gross and J. Meienhoffer, Eds), Vol IV. Academic Press, New York 1981.
43. Cremer D., Pople J.A.: J. Am. Chem. Soc. *97*, 1354 (1975).
44. Le Cocq C., Lallemand J.-Y.: J. Chem. Soc., Chem. Commun. *1981*, 150.
45. Davies D.B., Khaled A.: Tetrahedron Lett. *1973*, 2829.
46. Davies D.B., Khaled A.: J.Chem.Soc., Perkin Trans. 2 *1973*, 1651.
47. Haasnoot C.A.G., de Leeuw F.A.A.M., Altona C.: Tetrahedron *36*, 2783 (1980).
48. Huggins M.L.: J. Am. Chem. Soc. *75*, 4123 (1953).
49. Maloň P., Frič I., Tichý M., Bláha K.: Collect.Czech. Chem. Commun. *42*, 3104 (1977).
50. Woody R.W. in: *Proceedings of the 1st International Conference on Circular Dichroism*, p.270. Bulgarian Academy of Sciences, Sofia 1985.
51. Nafie L.A., Freedman T.B.: Top. Stereochem. *17*, 113 (1987); and references therein.
52. Maloň P., Keiderling T.A.: Unpublished results.
53. Schellman J.A.: J. Chem. Phys. *58*, 2882 (1973); *60*, 343 (1974).
54. Warshel A. in: *Modern Theoretical Chemistry* (G.A. Segal, Ed.), Vol.8, p.133. Plenum, New York 1976; and references therein.
55. Singh R.D., Keiderling T.A.: J. Chem. Phys. *74*, 5347 (1981); J. Am. Chem. Soc. *103*, 2387 (1981).
56. Brooks B.R., Bruccoleri R.E., Olafson B.D., States D.J., Swaminathan S., Karplus M.: J. Comp. Chem. *4*, 187 (1983).
57. Nafie L.A., Keiderling T.A., Stephens P.J.: J. Am. Chem. Soc. *98*, 2715 (1976).
58. Laux L., Pultz V., Abbate S., Havel A., Overend J.A., Moscowitz A., Lightner D.A.: J. Am. Chem. Soc. *104*, 4276 (1982).

Translated by the author (P.M.).